CIVIL ENGINEERING JOURNAL

Article no. 40

THE CIVIL ENGINEERING JOURNAL 4-2025

PARAMETER ANALYSIS OF PRESTRESSED STEEL WIRE ROPE STRENGTHENED CONCRETE BEAMS

Xilong Zheng[1], Fang Jianhai[2] and Honglei Zhang[3]

1. *School of Intelligent and Architectural Engineering, Harbin University, No.109 Zhongxing Road, Harbin, Heilongjiang Province, China; Zhengxilong88@163.com*
2. *Guangzhou Beihuan Intelligent Transportation Technology Co., Ltd, Guangzhou 510030, China; 14777232468@163.com*
3. *Beijing Xinqiao Technology Development Co., Ltd, Bridges and Tunnels Department, Beijing, No.8 Xitucheng, PR of China; Hongleizhang_Xq@163.com*

Received: *28.05.2025*
Received in revised form: *28.10.2025*
Accepted: *24.11.2025*

ABSTRACT

This paper systematically analyzes the parameters of prestressed steel wire rope strengthened concrete beams using finite element software ANSYS, aiming to explore the influence of different reinforcement parameters on the flexural performance of the beams. Seven 2.4m concrete beam models with different reinforcement methods were established, including comparisons of factors such as the number of prestressed tendons, tensile control stress, and composite mortar protection. Through simulated loading tests, the deflection changes, stress distribution, and force characteristics of steel bars and steel strands were examined. The results indicate that prestressed reinforcement significantly improves the stress state of the beams: an increase in prestress can effectively reduce the tensile stress at the beam bottom and decrease the stress in the main reinforcement, but has no significant impact on structural stiffness. An increase in the cross-sectional area of prestressed tendons significantly enhances the beam's stiffness. Composite mortar protection, although increasing self-weight, reduces prestress loss and optimizes the stress distribution of the steel strands. In contrast, the steel plate bonding method fails to fully utilize its effectiveness under low loads and even increases the stress in the steel bars. Additionally, excessively high prestress values may lead to excessive tensile stress at the beam bottom, necessitating reasonable design in practical engineering. This study provides a theoretical basis and parameter optimization directions for the engineering application of prestressed steel wire rope strengthened concrete beams, verifying the effectiveness of this technology in enhancing bridge load-carrying capacity and extending service life.

KEYWORDS

Prestressed steel wire rope, Concrete beam strengthening, Finite element analysis, Parameter optimization, Flexural performance, Composite mortar

INTRODUCTION

Early-built bridges, designed with lower load standards, are still in service on most highways

and bridges, but they no longer meet the increasing traffic demands. Therefore, the task of reinforcing and repairing dilapidated bridges is heavy. The idea of complete reconstruction is neither practical nor scientific [1-3]. Practice has proven that adopting appropriate reinforcement techniques and widening measures can restore and enhance the load-carrying capacity and traffic capacity of old bridges, extending their service life to meet the needs of modern transportation [4].

The reinforcement and repair of old bridges are technically feasible and economically reasonable initiatives, but they also face many practical difficulties, such as difficulty in finding original bridge data, lack of funds, and mature technical support, making bridge reinforcement difficult to carry out [5-9]. Since reinforcing old bridges is like performing surgery on a critically ill patient, it is risky and not highly profitable. Additionally, each bridge's condition varies greatly, making generalization difficult, which discourages capable survey, design, and construction units from getting involved, resulting in a situation where bridge reinforcement and reconstruction are in demand but not widely undertaken [10-12].

There are many methods for bridge reinforcement, such as increasing the section area, bonding steel beams, and bonding composite fibers. However, these methods have significant limitations, often resulting in strain lag effects during the reinforcement design process, failing to fully utilize the properties of the reinforcement materials. Therefore, these methods are collectively referred to as passive reinforcement methods [13-16].

Adopting active reinforcement methods by applying prestress to the structure can effectively utilize the reinforcement materials and greatly improve the reinforcement effect, solving the strain lag effect caused by staged loading in passive reinforcement. Using composite mortar steel strand bonded prestressed reinforcement for bridge components can effectively address the strain lag effect [17-19]. Due to its convenient prestress tensioning, simple anchoring structure, and high structural durability, it has attracted attention in the engineering community. Currently, only experimental studies have been conducted on prestressed steel wire rope strengthened beams. Liu and Wu [20,21] conducted a large-scale bending test on concrete beams reinforced with prestressed steel wire ropes to study the effects of the steel wire rope reinforcement ratio, reinforcement method, and the unbonded length at the interface between the steel wire rope and polymer mortar on the bending resistance of concrete beams. The test results show that the proposed reinforcement technology can significantly improve the load-bearing capacity of reinforced concrete beams.

Although there have been studies on the scale-down test of reinforced beams, there are few studies on the finite element simulation of prestressed wire rope reinforced beams. This paper conducts finite element simulation and parameter analysis of prestressed steel wire rope strengthened beams based on experimental data.

FINITE ELEMENT MODEL ESTABLISHMENT

Element Selection

ANSYS software has comprehensive pre- processing and post-processing functions, as well as powerful graphics and data processing capabilities, making it convenient to simulate the stress conditions of various parts of the bridge and achieve simulation analysis of bridge design calculations. The reinforced concrete beam is modeled using solid modeling, with different elements selected for C30 concrete, composite mortar, HRB235 steel bars, and steel strands. ANSYS provides multiple element options, with SOLID65 (reinforced concrete solid element) selected for the concrete unit in this model, which has three translational degrees of freedom. The steel bar and steel strand units use LINK8 elements, a type of truss element that only bears axial force and not bending moment, similar to the stress conditions of steel bars and steel strands, with nodes also having three translational degrees of freedom. Although SOLID65 could be used for steel bars and steel strands as well, due to the thin thickness of the composite mortar (typically 3-5cm) and its application only

to the beam bottom to bear tensile stress, the SHELL41 element is used for more accurate simulation in this model.

Connection Method of Composite Mortar and Beam Body

In actual reinforcement, composite mortar is applied to the beam bottom after prestress is applied, bonding with the steel wire ropes into an integral whole. When the beam is subjected to load and deformation, the mortar and the beam bottom concrete have the same displacement (Ux, Uy, Uz). Therefore, the CFINTF (coincident node coupling) command is used to couple the degrees of freedom of the concrete beam bottom nodes and the mortar nodes, forcing them to have the same displacement to simulate the connection between the composite mortar and the beam body.

Parameter Selection

This model simulates a 2.4 m reinforced concrete rectangular beam, with basic parameters matching those of the beam in the indoor small-scale beam test. The parameters of concrete and steel bars are shown in Table 1.

Tab.1 - Material Parameters Table

Material Name	Elastic Modulus (MPa)	Poisson's Ratio	Equivalent Weight (kg/m³)
Main Beam Concrete	$3.00e^4$	0.2	2500
Steel Bars	$2.00\ e^5$	0.3	7800
Steel Wire Ropes	$1.95\ e^5$	0.3	7800
Composite Mortar	$3.00\ e^5$	0.3	2500

The main beam concrete is modeled using SOLID65 elements, while steel bars and steel wire ropes are modeled using LINK8 elements. After meshing the structure, the finite element models are shown in Figures 1 and 2.

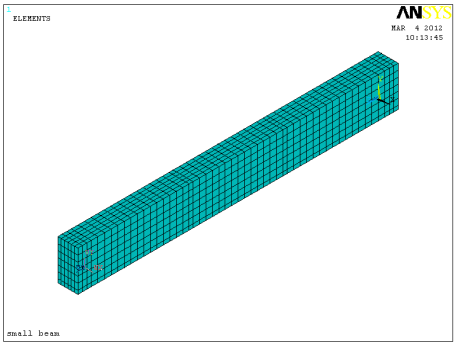

Fig. 1 - Concrete Meshing

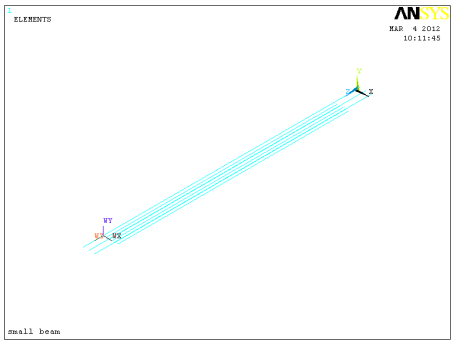

Fig.2 - Steel Bar Meshing

The composite mortar is modeled using SHELL41 elements, located at the beam bottom with a longitudinal range of 0.2 m-2.2 m and a thickness of 3cm, meshed similarly to the concrete. To simulate the bonding between the mortar and the beam bottom, the corresponding nodes of the beam bottom concrete and the composite mortar are coupled in the Ux, Uy, and Uz directions, as shown in Figures 3 and 4.

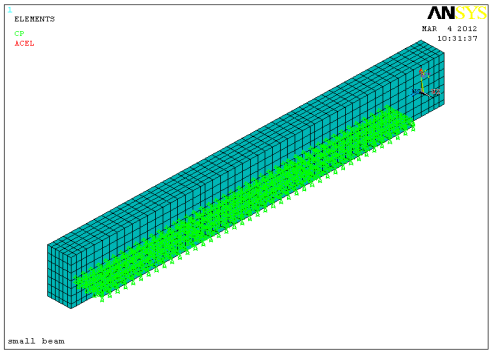

Fig. 3 - Mortar Simulation Reinforcement

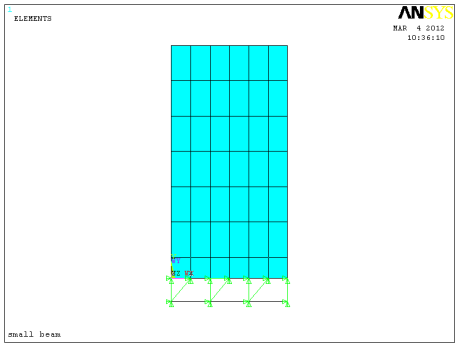

Fig. 4 - Mortar and Beam Bottom Connection Method

To achieve a pure bending state at the mid-span, a two-point loading method is used, applying two surface loads at the beam top. Since the structure is a simply supported beam, the supports are located 100.5 mm from the beam ends, with linear constraints applied.

This model analysis mainly investigates several influencing factors of the bonded prestressed reinforcement system: the cross-sectional area of prestressed steel bars, the contribution of composite mortar to beam stiffness, and the effect of tensile control stress on the reinforcement system. A total of seven models are established, as shown in Table 2.

Tab. 2 - Reinforcement Methods for Each Beam

Beam Number	Reinforcement Method	Prestress Description	Covering Layer
A1	Comparison Beam	Original Beam	No
B1	5 Steel Wire Ropes	Tensile Control Stress 835MPa	Mortar
B2	5 Steel Wire Ropes	Tensile Control Stress 835MPa,	No
C1	8 Steel Wire Ropes	Tensile Control Stress 835MPa	Mortar
C2	8 Steel Wire Ropes	Tensile Control Stress 1002MPa	Mortar

FLEXURAL PERFORMANCE ANALYSIS OF REINFORCED BEAMS

Model Deflection Analysis

The calculated values of this model serve as theoretical values for the small-scale beam reinforcement test in the past. Therefore, the same loading values as the test are applied to each beam at different levels, and the deflections of the beams are analyzed. The deflections of each beam under load are shown in Figures 5 and 6.

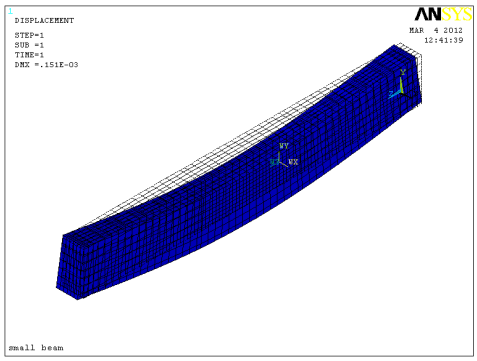

Fig.5 - Beam Deflection Under Load

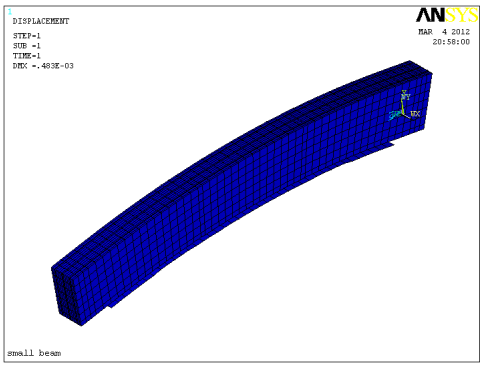

Fig.6 - Beam Camber Under Prestress

Tables 3-6 show the deflection values of each beam at various load levels (mm).

Tab.3 - Deflection Values of Each Beam at Various Load Levels Table 1 (mm)

Beam Number	Loading Value (kN)						
	0	3.3	6.6	9.9	13.2	14	14.8
	Deflection (mm)						
Beam A1	0.000	0.095	0.19	0.285	0.38	0.403	0.426
Beam B1	-0.193	0.077	0.154	0.234	0.311	0.33	0.349
Beam B2	-0.262	0.093	0.186	0.281	0.375	0.397	0.42
Beam C1	-0.320	0.077	0.154	0.23	0.32	0.33	0.35
Beam C2	-0.424	0.077	0.154	0.231	0.307	0.326	0.344
Beam C3	-0.493	0.077	0.18	0.253	0.285	0.293	0.3
Beam D1	0.077	0.152	0.226	0.301	0.376	0.394	0.412

Tab.4 - Deflection Values of Each Beam at Various Load Levels Table 2 (mm)

Beam Number	Loading Value (kN)						
	15.6	16.5	27.5	38.5	49.5	60.5	71.5
	Deflection (mm)						
Beam A1	0.449	0.475	0.792	1.109	1.426	1.743	2.06
Beam B1	0.443	0.468	0.78	1.092	1.404	1.716	2.028
Beam B2	0.443	0.468	0.78	1.092	1.404	1.716	2.028
Beam C1	0.37	0.39	0.642	0.899	1.156	1.413	1.669
Beam C2	0.363	0.38	0.643	0.9	1.156	1.413	1.67
Beam C3	0.308	0.316	0.781	1.082	1.386	1.691	1.996
Beam D1	0.43	0.45	0.699	0.948	1.197	1.445	1.694

Tab.5 - Deflection Values of Each Beam at Various Load Levels Table 3 (mm)

Beam Number	Loading Value (kN)						
	82.5	93.5	106	111.2	116	126	136
	Deflection (mm)						
Beam A1	2.377	2.693	3.054	3.342	/	/	/
Beam B1	1.943	2.202	2.496	2.732	2.967	3.203	3.438
Beam B2	2.34	2.652	3.007	3.29	3.574	3.857	4.141
Beam C1	1.926	2.183	2.475	2.708	2.942	3.175	3.408
Beam C2	1.926	2.183	2.475	2.708	2.942	3.175	3.409
Beam C3	2.301	2.607	2.954	3.232	3.363	3.51	3.788
Beam D1	1.943	2.192	2.474	2.7	2.809	/	/

Tab.6 - Deflection Values of Each Beam at Various Load Levels Table 4 (mm)

Beam Number	Loading Value (kN)						
	146	150	160	165.2	180	186	196.2
	Deflection (mm)						
Beam A1	/	/	/	/	/	/	/
Beam B1	3.758	/	/	/	/	/	/
Beam B2	/	/	/	/	/	/	/
Beam C1	3.502	3.735	3.857	/	/	/	/
Beam C2	3.502	3.735	3.857	4.202	4.342		
Beam C3	4.066	4.177	4.455	4.6	5.011	5.178	5.461
Beam D1	/	/	/	/	/	/	/

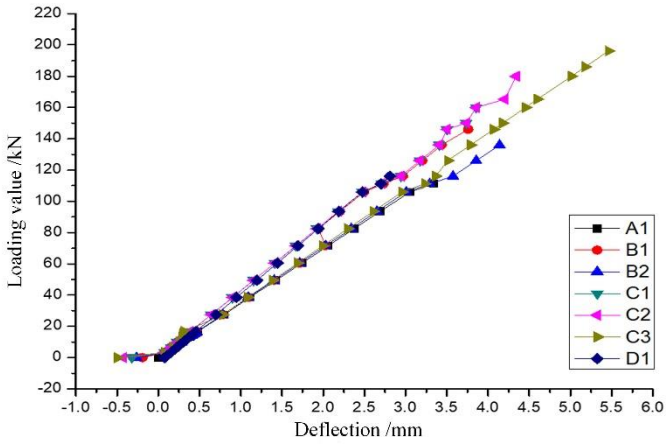

Fig.7 - Beam Deflection Values at Various Load Levels

Beam deflection values at various load levels Figure 7. From the deflection data, the following conclusions can be drawn:

(1) The five beams (B, C) reinforced with prestressed steel wire ropes exhibit camber values (deflections under zero load) of 0.193 mm, 0.262 mm, 0.32 mm, 0.424 mm, and 0.493 mm, respectively, with the camber value proportional to the applied prestress value. The camber value of

beam B2 without mortar is 54% higher than that of beam B1, indicating that the application of mortar significantly affects the initial camber value of the reinforced beam.

(2) The load-deflection curves of all beams initially grow linearly and then decline in the later stage. Before cracking, the concrete beams behave elastically; with the growth of cracks, the beams enter the plastic stage.

(3) By comparing the C1~C3 curves, it is found that under each load level, the deflections produced by the beams are almost identical, indicating that the influence of the bonded prestressed reinforcement system on beam stiffness is related to the area of the steel strands and independent of the initial tensile control stress. The tensile force only changes the internal stress state of the concrete beam, reducing the tensile stress of the steel bars and the tensile stress at the bottom edge of the concrete; it has no significant impact on the stiffness of the structure. The steel wire ropes act as ordinary steel bars.

(4) According to the D1 curve, the steel plate bonding method increases the structural stiffness by 17.9%, while the bonded prestressed reinforcement method increases it by 19.8%-72.9%, showing a significant increase in stiffness.

Structural Stress Analysis

(1) Stress Analysis Under 6.6 kN Load

The strain cloud diagrams of the original and reinforced structures are shown in Figures 8-11.

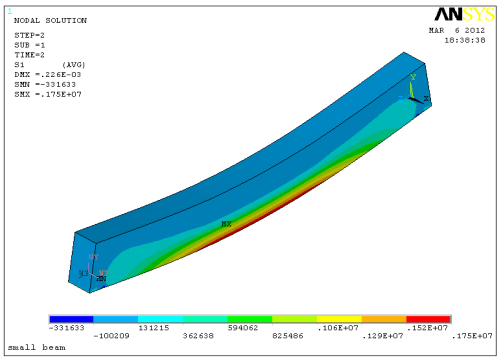

Fig.8 - Original Structure Concrete Strain Contour Diagram

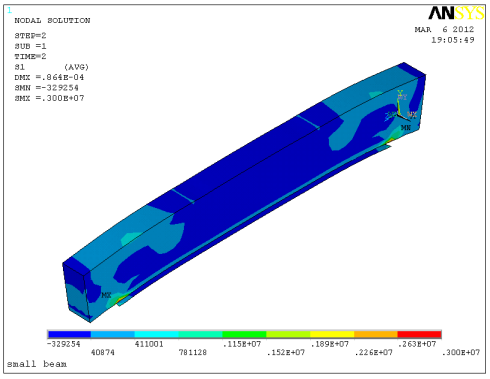

Fig.9 - B1 Concrete Strain Contour Diagram

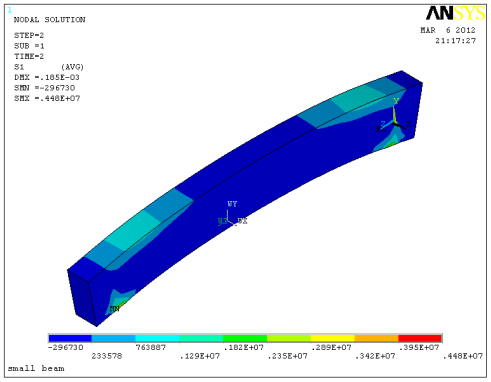

Fig. 10 - C1 Concrete Strain Contour Diagram

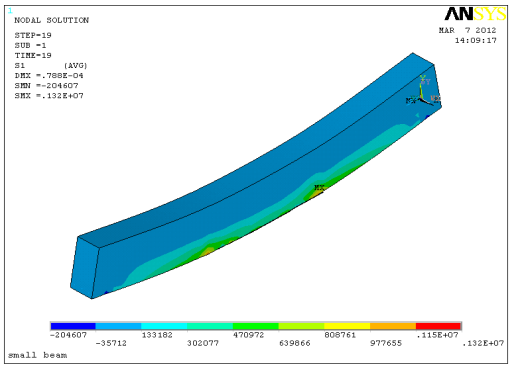

Fig. 11 - D1 Concrete Strain Contour Diagram

Under the action of the original structure and the reinforced structure, the main beam deflects

downward under load, generating corresponding tensile stress within the mid-span range of the beam bottom. The reinforced beam body exhibits smaller tensile stress compared to the original beam. In contrast, the actively reinforced beam body generates camber under small loads, with compressive stress at the beam bottom.

1) Concrete Stress Analysis at Mid-span Cross-section

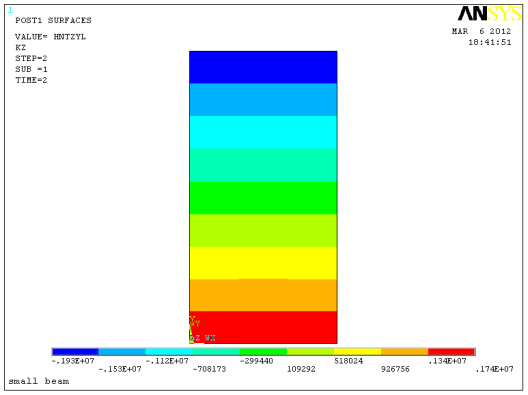

Fig.12 - A1 Mid-span Section Stress Contour Diagram

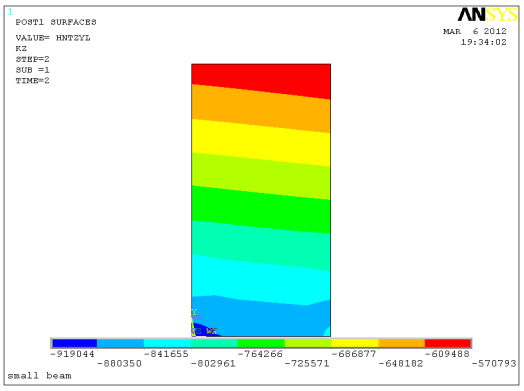

Fig.13 - B1 Mid-span Section Stress Contour Diagram

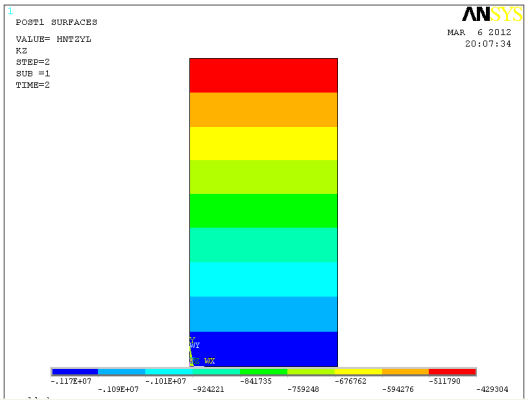

Fig.14 - B2 Mid-span Section Stress Contour Diagram

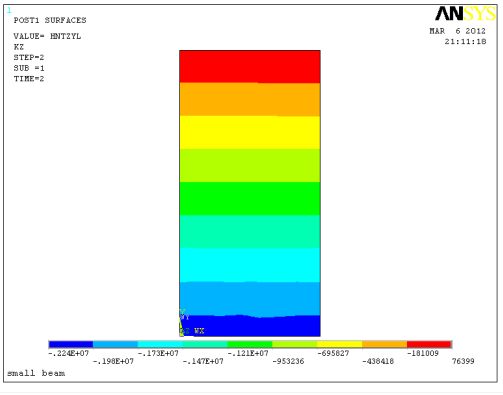

Fig.15 - C1 Mid-span Section Stress Contour Diagram

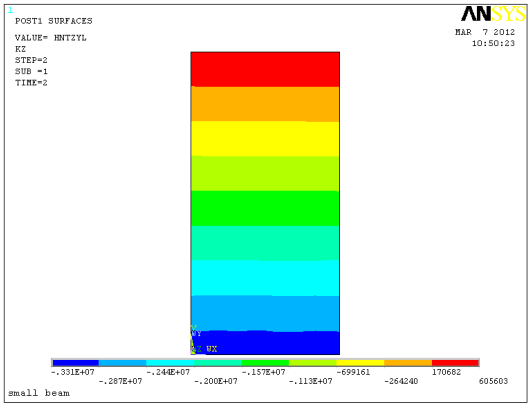

Fig.16 - C2 Mid-span Section Stress Contour Diagram

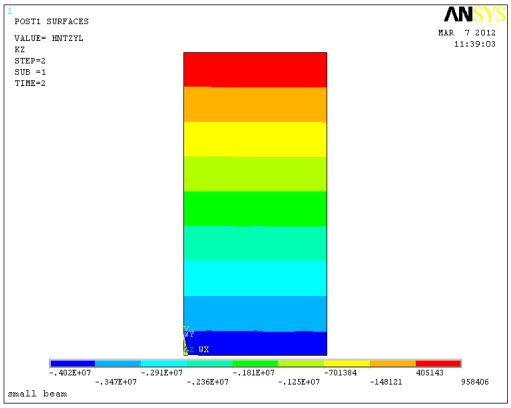

Fig.17 - C3 Mid-span Section Stress Contour Diagram

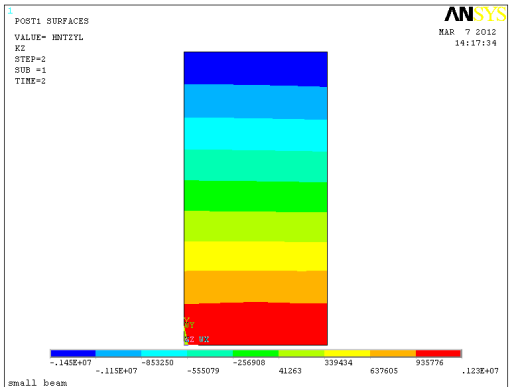

Fig.18 - D1 Mid-span Section Stress Contour Diagram

Tab.7 - Concrete Stress Data Analysis

Specimen Number	Top Edge Concrete Stress (MPa)	Bottom Edge Concrete Stress (MPa)	Top Edge Concrete Stress Ratio	Bottom Edge Concrete Stress Ratio
A1 B1	-3.78 -0.57	3.41 -0.92	1 0.15	1 -0.27
B2	-0.43	-1.17	0.11	-0.34
C1	0.08	-2.24	-0.02	-0.66
C2	0.61	-3.31	-0.16	-0.97
C3	0.96	-4.02	-0.25	-1.17
D1	-1.45	1.23	0.38	0.36

The stress cloud diagrams and data analysis of the mid-span cross-sections of each beam are shown in Figures 12-18 and Table 7. The passively reinforced beam (D1) generates tensile stress of 1.23MPa at the beam bottom, which is 36% of the original beam's stress, and compressive stress of -1.45 MPa at the beam top, which is 38% of the original beam's stress, indicating that the steel plate bonding method can reduce the concrete stress under external load. The actively reinforced beams (B, C) generate compressive stress at the beam bottom and tensile stress at the beam top, which is beneficial for the concrete's stress state and can delay crack development. The magnitude of the compressive stress at the beam bottom is proportional to the applied prestress value, increasing from -0.92 MPa to -4.02 MPa, showing better reinforcement effects compared to the steel plate bonding method.

2) Steel Bar Stress Analysis

Under external load, the main reinforcement bars within the structure bear tensile stress. When the tensile stress reaches the yield strength of the steel bars, the structure fails. Therefore, when studying the reinforcement system, reducing the tensile stress of the main reinforcement bars is a key condition for evaluating the load-carrying capacity improvement of the reinforcement system.

Tab.8 - Stress Data Analysis of Steel Bars and Steel Strands

Specimen Number	Midspan Steel Bar Stress (MPa)	Midspan Steel Wire Ropes Stress (MPa)	Mid-span Steel Bar Stress Ratio	Mid-span Steel Wire Ropes Stress Ratio
A1	9.42	/	1	/
B1	-9.32	-829	-0.99	/
B2	-17	827	-1.81	/
C1	-18.5	821	-1.96	/
C2	-24.6	1060	-2.61	/
C3	-28.8	1230	-3.06	/
D1	12.2	/	1.3	/

The stress data analysis of steel bars and steel wire ropes is shown in Table 8. The tensile stress of the original beam is 9.42 MPa. The actively reinforced method can significantly reduce the tensile stress of the main reinforcement bars, with an average tensile stress of -14.1 MPa for beam B, a reduction of 23.52 MPa, and -24 MPa for beam C, a reduction of 33.42 MPa. The reduction in tensile stress is proportional to the applied prestress value. In contrast, the passively reinforced beam D1 has a tensile stress of 12.2 MPa for the main reinforcement bars under a 6.6 kN load, 130% of the original beam's stress, indicating that under this load, the steel plate bonding method does not exert its reinforcement effect but increases the structure's self-weight, imposing additional load on the steel bars.

3) Stress Analysis of Steel Wire Ropes

The steel wire ropes, applied at the beam bottom, bear the bending moment induced by external loads together with the reinforced concrete. The steel wire ropes only bear tensile stress, and the stress values are shown in Figures 19-23. The tensile stress of the steel wire ropes increases under external load, and the stress is higher at the mid-span than at the beam ends, indicating that the deformation of the steel wire ropes is related to the position of the applied external load (and thus the structural deformation).

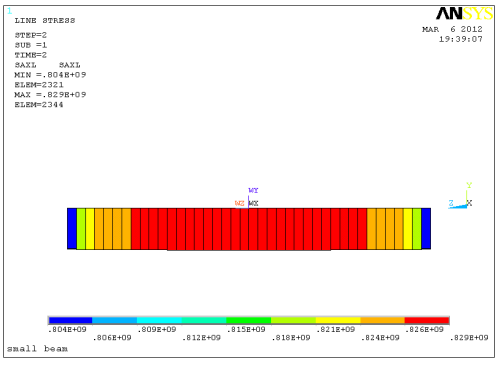

Fig.19 - B1 Steel Strand Strain Contour Diagram

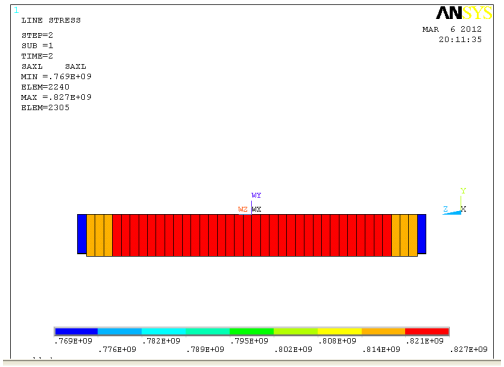

Fig.20 - B2 Steel Strand Strain Contour Diagram

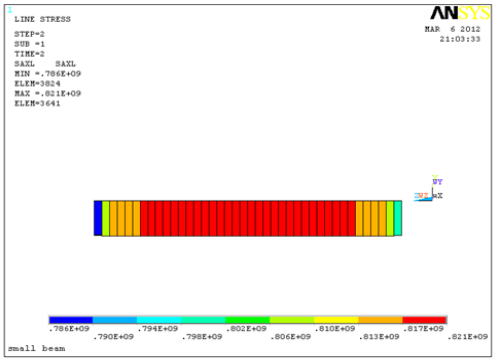

Fig.21 - C1 Steel Strand Strain Contour Diagram

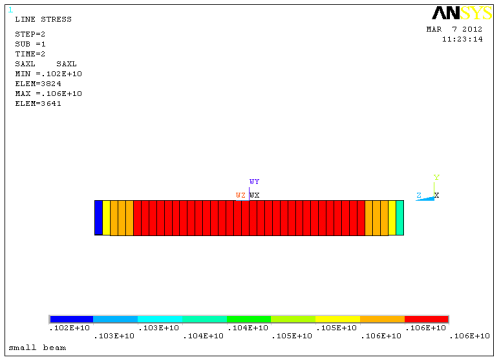

Fig.22 - C2 Steel Strand Strain Contour Diagram

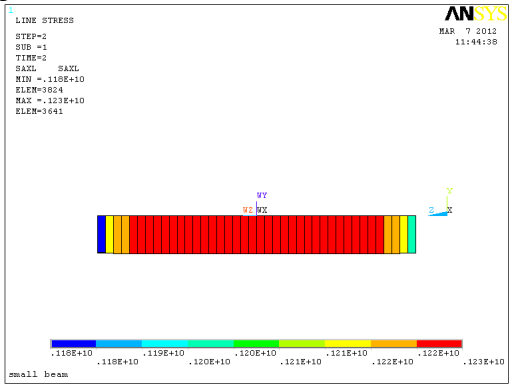

Fig.23 - C3 Steel Strand Strain Contour Diagram

(2) Stress Analysis Under 14 kN Load

A concentrated load of 14 kN is applied to each of the seven beams, generating a pure bending state at the mid-span. By analyzing the stress changes in the mid-span cross-section concrete, steel bars, and steel wire ropes, the stress state of the beams is obtained.

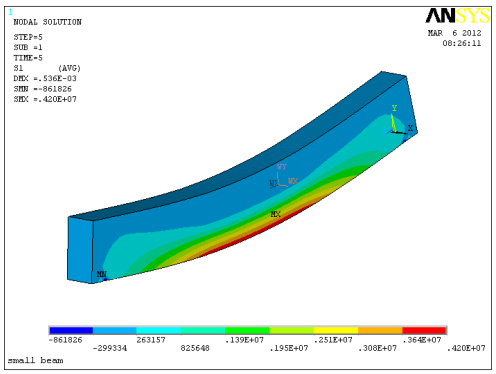

Fig.24 - Original Structure Concrete Strain Contour Diagram

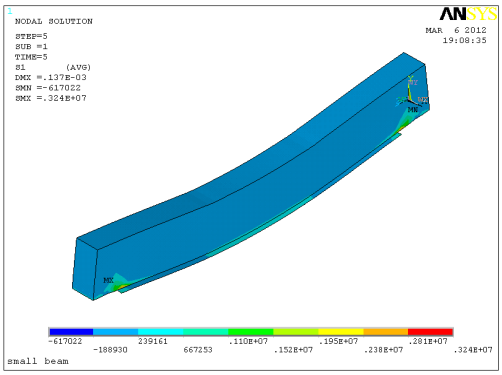

Fig.25 - B1 Concrete Strain Contour Diagram

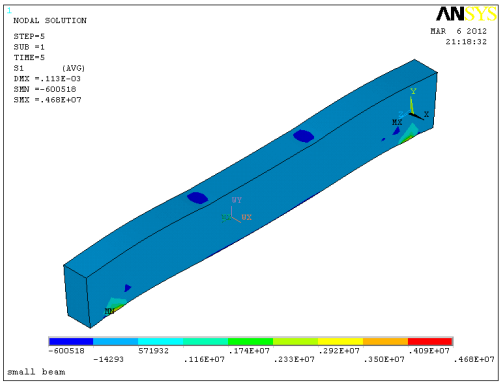

Fig.26 - C1 Concrete Strain Contour Diagram

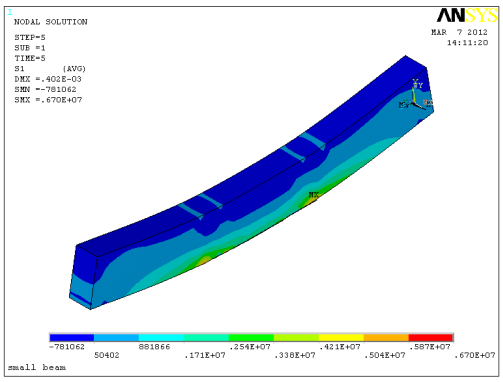

Fig.27 - D1 Concrete Strain Contour Diagram

Strain cloud diagrams of original and reinforced structures are shown in Figures 24-27. Under the action of the load, the original beam and the steel plate-reinforced beam deflect downward, generating corresponding tensile stress within the mid-span range of the beam bottom. The reinforced beam body exhibits smaller tensile stress compared to the original beam. In contrast, the actively reinforced beam body generates tensile stress at the beam bottom when the load exceeds the stress-relieving load, while the beam body does not exceed the stress-relieving load, generating compressive stress at the beam bottom.

1) Concrete Stress Analysis at Mid-span Cross-section

Tab. 9 - Concrete Stress Data Analysis

Specimen Number	Mid-span Steel Bar Stress (MPa)	Mid-span Steel Strand Stress (MPa)	Mid-span Steel Bar Stress Ratio	Mid-span Steel Wire Ropes Stress Ratio
A1	-4.61	4.17	1	1
B1	-2.2	0.35	0.48	0.08
B2	-2.26	0.46	0.49	0.11
C1	-1.54	-0.90	0.33	-0.21
C2	-1.01	-2.04	0.22	-0.49
C3	-0.66	-2.76	0.14	-0.66
D1	-2.51	2.14	0.54	0.36

The concrete stress data analysis is shown in Table 9. The stress ratio is the ratio of the stress of each beam to that of beam A1. The passively reinforced beam (D1) generates tensile stress of 2.14 MPa at the beam bottom under external load, 56.6% of the original beam's stress, and compressive stress of -2.51 MPa at the beam top, 66.4% of the original beam's stress, indicating that the steel plate bonding method can reduce the concrete stress under external load. The actively reinforced beam B generates tensile stress at the beam bottom under load, with an average value of 0.45 MPa, indicating that the concrete of beams B1 and B2 begins to bear tensile stress. The beam body of beam C is under compressive strain at the beam bottom, with an average compressive stress of -1.9 MPa, indicating that the stress state of the concrete in the bonded reinforcement system is related to the prestress loading value. The higher the prestress, the less likely the beam bottom is to generate tensile stress.

2) Steel Bar Stress Analysis

Steel bar strain is shown in Figures 28-34.

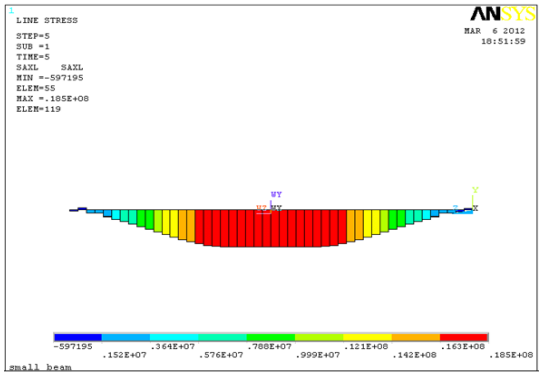

Fig.28 - Original Structure Steel Bar Strain Contour Diagram

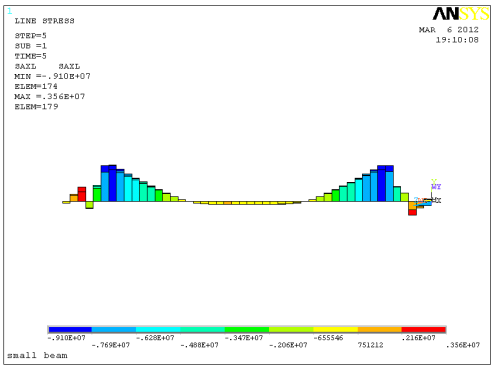

Fig.29 - B1 Steel Bar Strain Contour Diagram

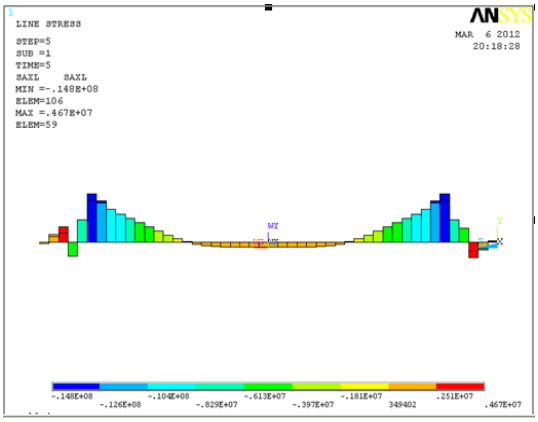

Fig.30 - B2 Steel Bar Strain Contour Diagram

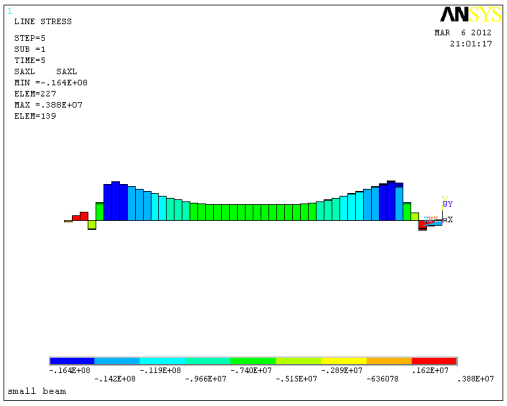

Fig.31 - C1 Steel Bar Strain Contour Diagram

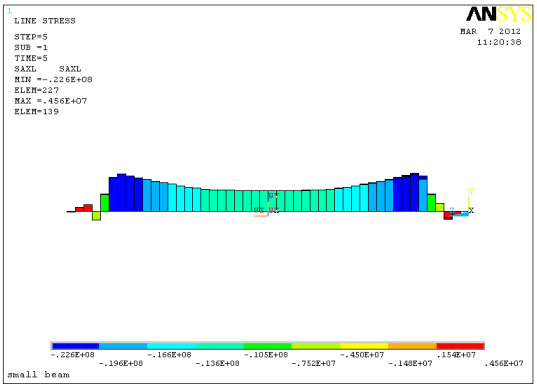

Fig.32 - C2 Steel Bar Strain Contour Diagram

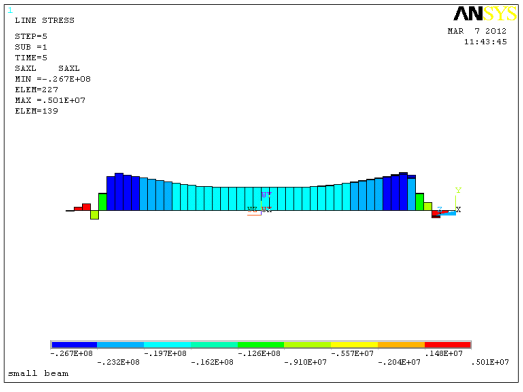

Fig.33 - C3 Steel Bar Strain Contour Diagram

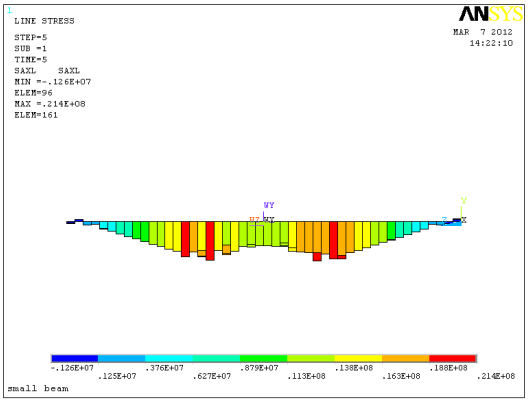

Fig.34 - D1 Steel Bar Strain Contour Diagram

Tab.10 - Stress Data Analysis of Steel Bars and Steel Wire Ropes

Specimen Number	Mid-span Steel Bar Stress (MPa)	Mid-span Steel Wire Ropes Stress (MPa)	Mid-span Steel Bar Stress Ratio	Mid-span Steel Strand Stress Ratio
A1	18.5	/	1	/
B1	-9.32	-837	-0.5	/
B2	-14.8	838	-0.8	/
C1	-16.4	829	-0.89	/
C2	-22.6	1070	-1.22	/
C3	-26.7	1240	-1.44	/
D1	21.4	/	1.16	/

The stress data analysis of steel bars and steel wire ropes is shown in Table 10. The tensile stress of the original beam is 18.5 MPa. The actively reinforced method can significantly reduce the tensile stress of the main reinforcement bars, with an average tensile stress of -12.1 MPa for beam B, a reduction of 30.6 MPa, and -21.9 MPa for beam C, a reduction of 40.4 MPa. The reduction in tensile stress is proportional to the applied prestress value. In contrast, the passively reinforced beam D1 has a tensile stress of 21.4 MPa for the main reinforcement bars, higher than the original beam, indicating that under a 14 kN load, the steel plate bonding method does not exert its reinforcement effect but increases the structure's self-weight, imposing additional load on the steel bars.

3) Stress Analysis of Steel Strands

Strain cloud diagrams of steel wire ropes are shown in Figures 35-39.

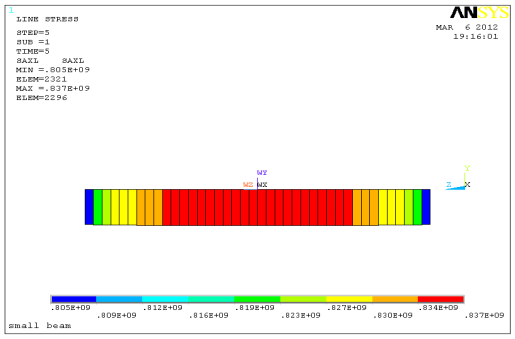

Fig.35 - B1 Steel Strand Strain Contour Diagram

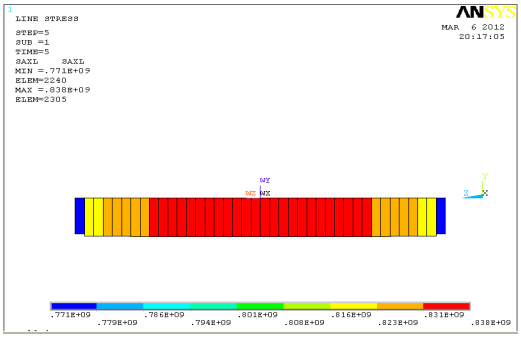

Fig.36 - B2 Steel Strand Strain Contour Diagram

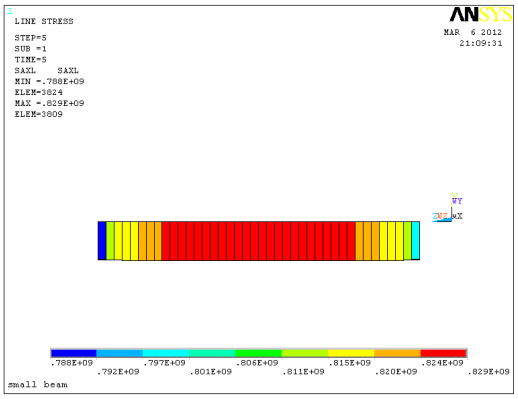

Fig.37 - C1 Steel Wire Ropes Strain Contour Diagram

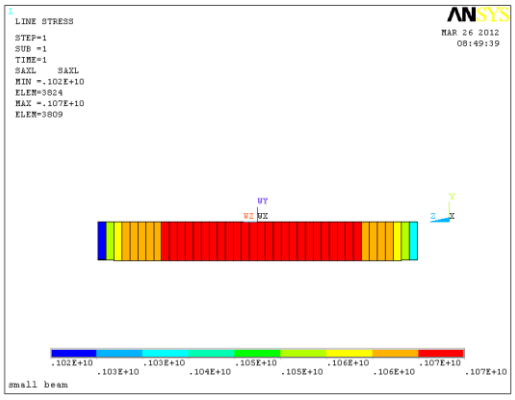

Fig.38 - C2 Steel Wire Ropes Strain Contour Diagram

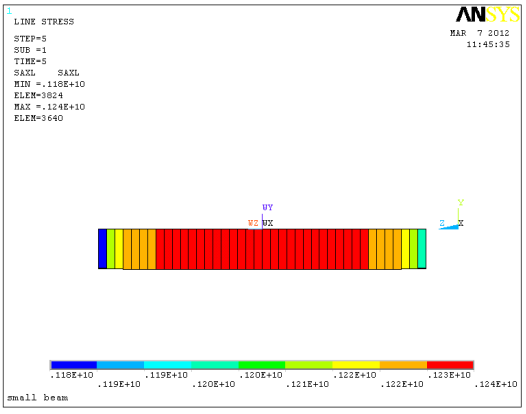

Fig.39 - C3 Steel Wire Ropes Strain Contour Diagram

Strain cloud diagrams of steel wire ropes are shown in Figures 35-39. Under external load, the tensile stress of the steel strands increases. The stress is higher at the mid-span than at the beam ends, indicating that the deformation of the steel wire ropes is related to the position of the applied external load (and thus the structural deformation).

CONSTRUCTION AND ECONOMIC ANALYSIS

1) Construction convenience analysis

The construction process is relatively simple: The construction process of prestressed steel wire rope reinforcement for Bridges is not complicated. It mainly includes the production of end anchors, the fixation of end anchor seats, the cutting of prestressed steel wire ropes and the production of extruded anchor heads, as well as the tensioning and anchoring of prestressed steel wire ropes. Compared with some traditional reinforcement methods such as the section enlargement reinforcement method, it does not require a large amount of concrete pouring and formwork erection work, and the construction process is relatively simplified.

The equipment requirements are not high: When tensioning prestressed steel wire ropes, since the tensile force of a single steel wire rope is relatively small, there is no need for large-scale tensioning equipment. Ordinary small tensioning tools can meet the requirements. This makes the preparation and operation of construction equipment more convenient, reducing the investment and usage difficulty of construction equipment.

Low requirements for on-site environment: This reinforcement method can achieve no wet operation or local wet operation, and has relatively low requirements for the environmental conditions of the construction site. In some bridge reinforcement scenarios with limited space or complex environments, such as Bridges in urban centers or those with small space under the bridge, prestressed steel wire rope reinforcement is easier to implement and can adapt to different construction site conditions.

Fast construction speed: The external prestressed reinforcement technology requires simple equipment, less human input, and a short construction period. Prestressed steel wire rope reinforcement is a type of external prestressed reinforcement. Its construction process is relatively efficient and can complete the bridge reinforcement work in a short time, reducing the impact on traffic.

2) Economy analysis

Low material cost: Prestressed steel wire ropes typically use high-strength, low-relaxation, and high-ductility steel wire ropes, and their material prices are relatively lower than those of some high-performance fiber composite materials and other reinforcing materials. Moreover, the diameter of steel wire ropes is generally small, and the amount of materials required is also relatively less, further reducing material costs.

Low construction cost: Due to the simple construction process, low equipment requirements, less labor input and short construction period, the construction cost of prestressed steel wire rope reinforced bridges is relatively low. Compared with methods such as reinforcing by pasting steel plates, it does not require a large amount of structural adhesives and also reduces the rework costs caused by problems such as bonding damage.

Low maintenance cost: Prestressed steel wire rope reinforcement basically does not increase the self-weight of the structure, does not reduce the usable space under the bridge, and the surface of the steel wire rope can be protected by applying protective mortar and other methods, which has good durability and is less likely to cause corrosion and other problems, thereby reducing the maintenance cost of the bridge in the subsequent use process.

High comprehensive economic benefits: Although prestressed steel wire rope reinforcement of bridges may require certain investment in the initial stage, in the long run, its relatively low construction cost, maintenance cost, and the ability to effectively enhance the load-bearing capacity and service life of Bridges make its comprehensive economic benefits quite significant, providing an economical and effective solution for the reinforcement and maintenance of bridges.

CONCLUSIONS

By establishing seven ANSYS small-scale beam models and analyzing the deformation and stress changes of each beam under different loads, the following conclusions are drawn:

(1) Through structural stress analysis, it is known that the prestress value applied by the prestressed wire ropes (tested at 50%-70% of the tensile control stress) can effectively improve the stress distribution of the structure, generating compressive stress at the beam bottom interface and tensile stress at the beam top interface, reducing the tensile stress of the main steel bars and increasing the maximum load-carrying capacity of the structure. However, the prestress value does not affect the stiffness of the structure.

(2) The cross-sectional area of the prestressed steel wire ropes can significantly change the structural stiffness. That is, under the same prestress level, the more prestressed steel wire ropes (lower tensile control stress), the greater the increase in structural stiffness, but the load-carrying capacity remains the same. The bonded prestressed reinforcement method increases it by 19.8%-72.9%, showing a significant increase in stiffness.

(3) When the prestressed steel wire ropes do not reach the ultimate tensile strength under ultimate conditions, the prestress level directly affects the load-carrying capacity of the structure. The higher the prestress level, the more significant the improvement in load-carrying capacity. Excessive prestress will cause excessive camber of the beam. Therefore, it is not advisable to adopt excessively high prestress values in actual reinforcement.

(4) The steel plate bonding method can increase the stiffness of the structure, but under small loads, the structure bears additional loads, and the steel bar stress values are higher than before reinforcement under the same load conditions. The reinforcement material does not exert its intended effect, only when loaded to a certain value does the structural stiffness improve to some extent.

REFERENCES

[1] Park Y H, Park C, Park Y G,. 2005. The behavior of an in-service plate girder bridge strengthened with external prestressing tendons. Engineering structures, vol. 27, n. 3, p. 379-386. ISSN: 0141-0296, https://doi.org/10.1016/j.engstruct.2004.10.014

[2] Miyamoto A, Tei K, Nakamura H,. 2000. Behavior of prestressed beam strengthened with external tendons. Journal of Structural Engineering, vol. 126, n. 9, p. 1033-1044. ISSN: 0733-9445, https://doi.org/10.1061/(ASCE)0733-9445(2000)126:9(1033)

[3] Reggia A, Morbi A, Plizzari G A,. 2020. Experimental study of a reinforced concrete bridge pier strengthened with HPFRC jacketing. Engineering Structures, vol. 210, p.110355. ISSN: 0141-0296, https://doi.org/10.1016/j.engstruct.2020.110355

[4] Hou P, Yang J, Pan Y,. 2022. Experimental and simulation studies on the mechanical performance of concrete T-Girder bridge strengthened with K-Brace composite trusses. Structures, vol. 43, p. 479-492. ISSN: 2352-0124, https://doi.org/10.1016/j.istruc.2022.06.069

[5] Czaderski C, Motavalli M,. 2007. 40-Year-old full-scale concrete bridge girder strengthened with prestressed CFRP plates anchored using gradient method. Composites Part B: Engineering, vol. 38, n. 7-8, p. 878-886. ISSN: 1359-8368, https://doi.org/10.1016/j.compositesb.2006.11.003

[6] Zampieri P, Simoncello N, Gonzalez-Libreros J,. 2020. Evaluation of the vertical load capacity of masonry arch bridges strengthened with FRCM or SFRM by limit analysis. Engineering Structures,vol. 225, p. 111135. ISSN: 0141-0296, https://doi.org/10.1016/j.engstruct.2020.111135

[7] Hu W, Li Y, Yuan H,. 2020. Review of experimental studies on application of FRP for strengthening of bridge structures. Advances in materials science and engineering, vol. 2020, n. 1, p. 8682163. ISSN: 1687-6822, https://doi.org/10.1155/2020/8682163

[8] Yang J, Hou P, Pan Y,. 2021. Shear behaviors of hollow slab beam bridges strengthened with high-performance self-consolidating cementitious composites. Engineering Structures, vol. 242, p. 112613. ISSN: 0141-0296, https://doi.org/10.1016/j.engstruct.2021.112613

[9] Schnerch D, Dawood M, Rizkalla S,. 2007. Proposed design guidelines for strengthening of steel bridges with FRP materials. Construction and building materials, vol. 21, n. 5, p. 1001-1010. ISSN: 950-0618, https://doi.org/10.1016/j.conbuildmat.2006.03.003

[10] Kang J, Wang X, Yang J,. 2013. Strengthening double curved arch bridges by using extrados section augmentation method. Construction and Building Materials, vol. 41, p. 165-174. ISSN: 950-0618, https://doi.org/10.1016/j.conbuildmat.2012.11.115

[11] Chen C, Yang C,. 2019. Experimental and simulation studies on the mechanical performance of T-girder bridge strengthened with transverse connection. Journal of Performance of Constructed Facilities, vol. 33, n. 5, p. 04019055. ISSN: 0887-3828, https://doi.org/10.1061/(ASCE)CF.1943-5509.0001318

[12] Zampieri P, Piazzon R, Niero L,. 2024. Damaged masonry arch bridges strengthened with external post-tensioning: Experimental and numerical results. Engineering Structures, vol. 318, p. 117929. ISSN: 0141-0296, https://doi.org/10.1016/j.engstruct.2024.117929

[13] Birajdar H S, Maiti P R, Singh P K,. 2016. Strengthening of Garudchatti bridge after failure of Chauras bridge. Engineering Failure Analysis, vol. 62, p. 49-57. ISSN: 1350-6307, https://doi.org/10.1016/j.engfailanal.2015.12.002

[14] Siwowski T, Piątek B, Siwowska P,. 2020. Development and implementation of CFRP post-tensioning system for bridge strengthening. Engineering Structures, vol. 207, p. 110266. ISSN: 0141-0296, https://doi.org/10.1016/j.engstruct.2020.110266

[15] Hou P, Yang J, Pan Y,. 2022. Experimental and simulation studies on the mechanical performance of concrete T-Girder bridge strengthened with K-Brace composite trusses. Structures, vol. 43, p. 479-492. ISSN: 2352-0124, https://doi.org/10.1016/j.istruc.2022.06.069

[16] Kim S H, Park J S, Jung W T,. 2021. Experimental study on strengthening effect analysis of a deteriorated bridge using external prestressing method. Applied Sciences, vol. 11, n. 6, p. 2478. ISSN: 1454-5101, https://doi.org/10.3390/app11062478

[17] Izadi M, Motavalli M, Ghafoori E,. 2019. Iron-based shape memory alloy (Fe-SMA) for fatigue strengthening of cracked steel bridge connections. Construction and Building Materials, vol. 227, p. 116800. ISSN: 0950-0618, https://doi.org/10.1016/j.conbuildmat.2019.116800

[18] Miao X, Li Z, Liu S,. 2023. Ionic bridging strengthened MXene/GO nanocomposite films with extraordinary mechanical and tribological properties. Applied Surface Science, vol. 625, p. 157181. ISSN: 0169-4332, https://doi.org/10.1016/j.apsusc.2023.157181

[19] Wang Z, Yang J, Zhou J,. 2022. Strengthening of existing stone arch bridges using UHPC: Theoretical analysis and case study. Structures, vol. 43, p. 805-821. ISSN: 2352-0124, https://doi.org/10.1016/j.istruc.2022.06.055

[20] Liu Z Q, Guo Z X, Ye Y,. 2022. Flexural behaviour of RC beams strengthened with prestressed steel wire ropes polymer mortar composite. Journal of Asian Architecture and Building Engineering, vol. 21, n. 1, P. 48-65. https://doi.org/10.1080/13467581.2021.1928508

[21] Wu G, Wu Z S, Jiang J B,. 2010. Experimental study of RC beams strengthened with distributed prestressed high-strength steel wire rope. Magazine of concrete research, vol. 62, n. 4, p. 253-265. https://doi.org/10.1680/macr.2010.62.4.253